

## Three-Quark Potential in SU(3) Lattice QCD

T. T. Takahashi,<sup>1</sup> H. Matsufuru,<sup>1</sup> Y. Nemoto,<sup>2</sup> and H. Suganuma<sup>3,1</sup>

<sup>1</sup>*RCNP, Osaka University, Mihogaoka 10-1, Osaka 567-0047, Japan*

<sup>2</sup>*YITP, Kyoto University, Kitashirakawa, Sakyo, Kyoto 606-8502, Japan*

<sup>3</sup>*Faculty of Science, Tokyo Institute of Technology, Tokyo 152-8551, Japan*

(Received 23 May 2000)

The static three-quark ( $3Q$ ) potential is studied in SU(3) lattice QCD with  $12^3 \times 24$  and  $\beta = 5.7$  at the quenched level. From the  $3Q$  Wilson loop,  $3Q$  ground-state potential  $V_{3Q}$  is extracted using the smearing technique for ground-state enhancement. With accuracy better than a few percent,  $V_{3Q}$  is well described by a sum of a constant, the two-body Coulomb term, and the three-body linear confinement term  $\sigma_{3Q} L_{\min}$ , with  $L_{\min}$  the minimal value of total length of color flux tubes linking the three quarks. Comparing with the  $Q$ - $\bar{Q}$  potential, we find a universal feature of the string tension,  $\sigma_{3Q} \approx \sigma_{Q\bar{Q}}$ , and the OGE result for Coulomb coefficients,  $A_{3Q} \approx \frac{1}{2}A_{Q\bar{Q}}$ .

DOI: 10.1103/PhysRevLett.86.18

PACS numbers: 12.38.Gc

In general, the three-body force is regarded as a residual interaction in most fields of physics. In QCD, however, the three-body force among three quarks is expected to be a “primary” force reflecting the SU(3)<sub>c</sub> gauge symmetry. Indeed, the three quark ( $3Q$ ) potential [1–3] is directly responsible for the structure and properties of baryons [4], similar to the relevant role of the  $Q$ - $\bar{Q}$  potential upon meson properties [5]. In contrast with a number of studies on the  $Q$ - $\bar{Q}$  potential using lattice QCD [6,7], there were only a few lattice QCD studies for the  $3Q$  potential done mainly more than 13 years ago [8–11]. (In Ref. [11], the author showed only a preliminary result on the equilateral-triangle case without enough analyses.) In Refs. [8,10,11], the  $3Q$  potential seemed to be expressed by a sum of two-body potentials, which supports the  $\Delta$ -type flux-tube picture [12]. On the other hand, Ref. [9] seemed to support the Y-type flux-tube picture [2,4] rather than the  $\Delta$ -type one. These controversial results may be due to the difficulty of the accurate measurement of the  $3Q$  ground-state potential in lattice QCD. For instance, in Refs. [8,10], the authors did not use the smearing for ground-state enhancement, and therefore their results may include serious contamination from the excited-state component.

The  $3Q$  static potential can be measured with the  $3Q$  Wilson loop, where the  $3Q$  gauge-invariant state is generated at  $t = 0$  and is annihilated at  $t = T$ , as shown in Fig. 1. Here the three quarks are spatially fixed in  $\mathbf{R}^3$  for  $0 < t < T$ . The  $3Q$  Wilson loop  $W_{3Q}$  is defined in a gauge-invariant manner as

$$W_{3Q} \equiv \frac{1}{3!} \varepsilon_{abc} \varepsilon_{a'b'c'} U_1^{aa'} U_2^{bb'} U_3^{cc'} \quad (1)$$

with  $U_k \equiv P \exp\{ig \int_{\Gamma_k} dx^\mu A_\mu(x)\}$  ( $k = 1, 2, 3$ ). Here  $P$  denotes the path-ordered product along the path denoted by  $\Gamma_k$  in Fig. 1. Similar to the derivation of the  $Q$ - $\bar{Q}$  potential from the Wilson loop, the  $3Q$  potential  $V_{3Q}$  is obtained as  $V_{3Q} = -\lim_{T \rightarrow \infty} \frac{1}{T} \ln \langle W_{3Q} \rangle$ .

Physically, the true ground state of the  $3Q$  system, which is of interest here, is expected to be expressed by

the flux tubes instead of the strings, and the  $3Q$  state which is expressed by the three strings generally includes many excited-state components such as flux-tube vibrational modes. Of course, if the large  $T$  limit can be taken, the ground-state potential would be obtained. However,  $\langle W_{3Q} \rangle$  decreases exponentially with  $T$ , and then the practical measurement of  $\langle W_{3Q} \rangle$  becomes quite severe for large  $T$  in lattice QCD simulations. Therefore, for the accurate measurement of the  $3Q$  ground-state potential  $V_{3Q}$ , the smearing technique for ground-state enhancement [1,13,14] is practically indispensable. However, this smearing technique was not applied to the past lattice QCD studies for  $V_{3Q}$  in Refs. [8,10], since the smearing technique was mainly developed after their works.

In this paper, we study the  $3Q$  ground-state potential  $V_{3Q}$  using the ground-state enhancement by the gauge-covariant smearing technique for the link variable in SU(3)<sub>c</sub> lattice QCD with the standard action with  $\beta = 5.7$  and  $12^3 \times 24$  at the quenched level [1]. We consider 16 patterns of the  $3Q$  configuration where the

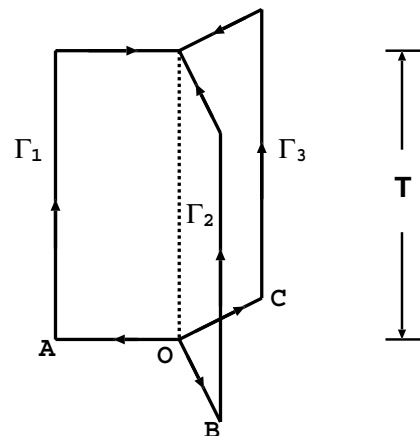


FIG. 1. The  $3Q$  Wilson loop  $W_{3Q}$ . The  $3Q$  state is generated at  $t = 0$  and is annihilated at  $t = T$ . The three quarks are spatially fixed in  $\mathbf{R}^3$  for  $0 < t < T$ .

three quarks are put on  $(i, 0, 0)$ ,  $(0, j, 0)$ , and  $(0, 0, k)$  in  $\mathbf{R}^3$  with  $0 \leq i, j, k \leq 3$  in the lattice unit. Here the junction point  $O$  is set at the origin  $(0, 0, 0)$  in  $\mathbf{R}^3$ , although the final result of the ground-state potential  $V_{3Q}$  should not depend on the artificial selection of  $O$ . For actual lattice QCD calculations of the  $3Q$  Wilson loop, we use the translational, the rotational, and the reflection symmetries on lattices on the choice of the origin  $O$  and the direction of  $\hat{x}, \hat{y}, \hat{z}$ .

The standard smearing for link variables is expressed as the iteration of the replacement of the spatial link variable  $U_i(s)$  ( $i = 1, 2, 3$ ) by the obscured link variable  $\bar{U}_i(s) \in \text{SU}(3)_c$  [13,14] which maximizes

$$\text{Re tr} \left\{ \bar{U}_i^\dagger(s) \left[ \alpha U_i(s) + \sum_{j \neq i} \{ U_j(s) U_i(s + \hat{j}) U_j^\dagger(s + \hat{i}) + U_j^\dagger(s - \hat{j}) U_i(s - \hat{j}) U_j(s + \hat{i} - \hat{j}) \} \right] \right\} \quad (2)$$

with the smearing parameter  $\alpha$  being a real number. The  $n$ th smeared link variables  $U_\mu^{(n)}(s)$  ( $n = 1, 2, \dots, N_{\text{smear}}$ ) are iteratively defined starting from  $U_\mu^{(0)}(s) \equiv U_\mu(s)$  as

$$U_i^{(n)}(s) \equiv \bar{U}_i^{(n-1)}(s) \quad (i = 1, 2, 3), \\ U_4^{(n)}(s) \equiv U_4(s). \quad (3)$$

As an important feature, this smearing procedure keeps the gauge covariance of the “fat” link variable  $U_\mu^{(n)}(s)$  properly. In fact, the gauge-transformation property of  $U_\mu^{(n)}(s)$  is just the same as that of the original link variable  $U_\mu(s)$ , and therefore the gauge invariance of  $F(U_\mu^{(n)}(s))$  is ensured whenever  $F(U_\mu(s))$  is a gauge-invariant function.

Since the fat link variable  $U_\mu^{(n)}(s)$  includes a spatial extension, the “line” expressed with  $U_\mu^{(n)}(s)$  physically corresponds to a “flux tube” with a spatial extension. Therefore, if a suitable smearing is done, the line of the fat link variable is expected to be close to the ground-state flux tube. (This smearing technique is actually successful for the extraction of the  $Q$ - $\bar{Q}$  potential in lattice QCD [14].)

Now we investigate the magnitude of the ground-state component in the  $3Q$ -state operator at  $t = 0, T$  in the  $3Q$  Wilson loop  $W_{3Q}$ . From the similar argument in the  $Q$ - $\bar{Q}$  system [14], the overlap of the  $3Q$ -state operator with the ground state is estimated with

$$C_0 \equiv \langle W_{3Q}(T) \rangle^{T+1} / \langle W_{3Q}(T+1) \rangle^T, \quad (4)$$

which we call the ground-state overlap. If the  $3Q$  state at  $t = 0, T$  in Fig. 1 is the perfect ground state,  $\langle W_{3Q}(T) \rangle = e^{-V_{3Q}T}$  and then  $C_0 = 1$  hold. [Here  $W_{3Q}(T)$  in Eq. (1) is normalized as  $\langle W_{3Q}(T=0) \rangle = 1$ .]

The ground-state potential  $V_{3Q}$  can be measured accurately if  $C_0$  is large enough. Then we check the ground-state overlap  $C_0$  of the  $3Q$  Wilson loop  $\langle W_{3Q}(U_\mu^{(n)}(s), T) \rangle$  composed of the fat link variable  $U_\mu^{(n)}(s)$  in lattice QCD

simulations, and search reasonable values of the smearing parameter  $\alpha$  and the iteration number  $N_{\text{smear}}$  for this purpose. In lattice QCD simulations, the ground-state overlap  $C_0$  is largely enhanced as  $0.8 < C_0 < 1$  for  $T \leq 3$  by the smearing with  $\alpha = 2.3$  and  $N_{\text{smear}} = 12$  for all of the  $3Q$  configurations in consideration, as shown in Fig. 2.

Here we make a theoretical consideration on the potential form in the  $Q$ - $\bar{Q}$  and  $3Q$  systems with respect to QCD. In the short-distance limit, perturbative QCD is applicable and the Coulomb-type potential appears as the one-gluon-exchange (OGE) result. In the long-distance limit at the quenched level, the flux-tube picture would be applicable from the argument of the strong-coupling limit of QCD [2,4,15], and hence a linear-type confinement potential proportional to the total flux-tube length is expected to appear. Of course, it is nontrivial that these simple arguments on the ultraviolet and infrared limits of QCD hold for the intermediate region as  $0.2 \text{ fm} < r < 1 \text{ fm}$ . Nevertheless, lattice QCD results for the  $Q$ - $\bar{Q}$  ground-state potential is well described by

$$V_{Q\bar{Q}}(r) = -\frac{A_{Q\bar{Q}}}{r} + \sigma_{Q\bar{Q}}r + C_{Q\bar{Q}} \quad (5)$$

at the quenched level [14]. Actually, we measure  $V_{Q\bar{Q}}$  from the on-axis Wilson loop with the smearing with  $\alpha = 2.3$  and  $N_{\text{smear}} = 20$ , and find a good fitting of Eq. (5) with the parameters  $(A_{Q\bar{Q}}, \sigma_{Q\bar{Q}}, C_{Q\bar{Q}})$  listed in Table I. (In general, the adequate values of  $\alpha$  and  $N_{\text{smear}}$  depend on the operator.) In fact,  $V_{Q\bar{Q}}$  is described by a sum of the short-distance OGE result and the long-distance flux-tube result.

Also for the  $3Q$  ground-state potential  $V_{3Q}$ , we try to apply this simple picture of the short-distance OGE result plus the long-distance flux-tube result. Then the  $3Q$  potential  $V_{3Q}$  is expected to take a form of

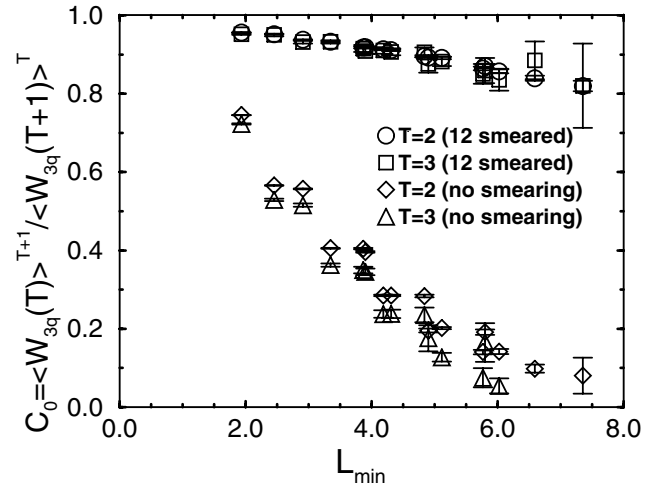


FIG. 2. The ground-state overlap of the  $3Q$  system,  $C_0 \equiv \langle W_{3Q}(T) \rangle^{T+1} / \langle W_{3Q}(T+1) \rangle^T$ , with the smeared link variable (upper data) and with unsmeared link variable (lower data). To distinguish the  $3Q$  system, we have taken the horizontal axis as  $L_{\min}$ , with the minimal length of the flux tubes linking the three quarks. For each  $3Q$  configuration,  $C_0$  is largely enhanced as  $0.8 < C_0 < 1$  by the smearing.

TABLE I. The coefficients in Eq. (6) for the  $3Q$  potential and those in Eq. (5) for the  $Q$ - $\bar{Q}$  potential in the lattice unit.

	$\sigma$	$A$	$C$
$3Q$	0.1524(28)	0.1331(66)	0.9182(213)
$Q$ - $\bar{Q}$	0.1629(47)	0.2793(116)	0.6203(161)

$$L_{\min} = \left[ \frac{1}{2} (a^2 + b^2 + c^2) + \frac{\sqrt{3}}{2} \sqrt{(a+b+c)(-a+b+c)(a-b+c)(a+b-c)} \right]^{1/2}, \quad (7)$$

when all angles of the  $3Q$  triangle do not exceed  $2\pi/3$ . In this case, there appears the physical junction which connects the three flux tubes originating from the three quarks, and the shape of the  $3Q$  system is expressed as a Y-type flux tube [4,15], where the angle between two flux tubes is found to be  $2\pi/3$  [2,4]. When an angle of the  $3Q$  triangle exceeds  $2\pi/3$ , one finds  $L_{\min} = a + b + c - \max(a, b, c)$ .

Now we show lattice QCD results for the  $3Q$  ground-state potential. We generate 210 gauge configurations using  $SU(3)_c$  lattice QCD Monte Carlo simulation with the standard action with  $\beta = 5.7$  and  $12^3 \times 24$  at the quenched level. The lattice spacing  $a \approx 0.19$  fm is determined so as to reproduce the string tension as  $\sigma = 0.89$  GeV/fm in the  $Q$ - $\bar{Q}$  potential  $V_{Q\bar{Q}}$ . Here the gauge configurations are taken every 500 sweeps after a thermalization of 5000 sweeps using the pseudo-heat-bath algorithm. In this study, lattice QCD calculations have been performed on NEC-SX4 at Osaka University.

We measure the  $3Q$  ground-state potential  $V_{3Q}$  using the smearing technique, and compare the lattice data with the theoretical form of Eq. (6). Owing to the smearing, the ground-state component is largely enhanced, and therefore

$$V_{3Q} = -A_{3Q} \sum_{i < j} \frac{1}{|\mathbf{r}_i - \mathbf{r}_j|} + \sigma_{3Q} L_{\min} + C_{3Q}, \quad (6)$$

where  $L_{\min}$  denotes the minimal value of total length of color flux tubes linking the three quarks. Denoting three sides of the  $3Q$  triangle by  $a$ ,  $b$ , and  $c$ ,  $L_{\min}$  is expressed as

the  $3Q$  Wilson loop  $\langle W_{3Q} \rangle$  composed with the smeared link variable exhibits a single-exponential behavior as  $\langle W_{3Q} \rangle \approx e^{-V_{3Q} T}$  even for a small value of  $T$ . Then, for each  $3Q$  configuration, we extract  $V_{3Q}^{\text{latt}}$  from the least squares fit with the single-exponential form

$$\langle W_{3Q} \rangle = \bar{C} e^{-V_{3Q} T} \quad (8)$$

in the range of  $T_{\min} \leq T \leq T_{\max}$  listed in Table II. Here we choose the fit range of  $T$  such that the stability of the “effective mass”  $V(T) \equiv \ln\{\langle W_{3Q}(T) \rangle / \langle W_{3Q}(T+1) \rangle\}$  is observed in the range of  $T_{\min} \leq T \leq T_{\max} - 1$ .

For each  $3Q$  configuration, we summarize the lattice data  $V_{3Q}^{\text{latt}}$  as well as the prefactor  $\bar{C}$  in Eq. (8), the fit range of  $T$  and  $\chi^2/N_{\text{DF}}$  in Table II. The statistical error of  $V_{3Q}^{\text{latt}}$  is estimated with the jackknife method. We find again a large ground-state overlap as  $\bar{C} > 0.8$  for all  $3Q$  configurations.

Now we consider the potential form. In Fig. 3, we plot the  $3Q$  ground-state potential  $V_{3Q}$  as the function of  $L_{\min}$ . Apart from a constant,  $V_{3Q}$  is almost proportional to  $L_{\min}$  in the infrared region. We show in Table I the best fitting parameters in Eq. (6) for  $V_{3Q}$ . On the goodness of this

TABLE II. Lattice QCD results for the  $3Q$  potential  $V_{3Q}^{\text{latt}}$  for 16 patterns of the  $3Q$  system, where the three quarks are put on  $(i, 0, 0)$ ,  $(0, j, 0)$ , and  $(0, 0, k)$  in  $\mathbf{R}^3$  in the lattice unit. For each  $3Q$  configuration,  $V_{3Q}^{\text{latt}}$  is measured from the single-exponential fit  $\langle W_{3Q} \rangle = \bar{C} e^{-V_{3Q} T}$  in the range of  $T$  listed at the fourth column. The statistical errors listed are estimated with the jackknife method, and  $\chi^2/N_{\text{DF}}$  is listed at the fifth column. The fitting function  $V_{3Q}^{\text{fit}}$  in Eq. (6) with the best fitting parameters in Table I is also added.

$(i, j, k)$	$V_{3Q}^{\text{latt}}$	$\bar{C}$	Fit range of $T$	$\chi^2/N_{\text{DF}}$	$V_{3Q}^{\text{fit}}$	$V_{3Q}^{\text{latt}} - V_{3Q}^{\text{fit}}$
(0, 1, 1)	0.8457( 38)	0.9338(173)	5–10	0.062	0.8524	−0.0067
(0, 1, 2)	1.0973( 43)	0.9295(161)	4–8	0.163	1.1025	−0.0052
(0, 1, 3)	1.2929( 41)	0.8987(110)	3–7	0.255	1.2929	0.0000
(0, 2, 2)	1.3158( 44)	0.9151(120)	3–6	0.053	1.3270	−0.0112
(0, 2, 3)	1.5040( 63)	0.9041(170)	3–6	0.123	1.5076	−0.0036
(0, 3, 3)	1.6756( 43)	0.8718( 73)	2–5	0.572	1.6815	−0.0059
(1, 1, 1)	1.0238( 40)	0.9345(149)	4–8	0.369	1.0092	0.0146
(1, 1, 2)	1.2185( 62)	0.9067(228)	4–8	0.352	1.2151	0.0034
(1, 1, 3)	1.4161( 49)	0.9297(135)	3–7	0.842	1.3964	0.0197
(1, 2, 2)	1.3866( 48)	0.9012(127)	3–7	0.215	1.3895	−0.0029
(1, 2, 3)	1.5594( 63)	0.8880(165)	3–6	0.068	1.5588	0.0006
(1, 3, 3)	1.7145( 43)	0.8553( 76)	2–6	0.412	1.7202	−0.0057
(2, 2, 2)	1.5234( 37)	0.8925( 65)	2–5	0.689	1.5238	−0.0004
(2, 2, 3)	1.6750(118)	0.8627(298)	3–6	0.115	1.6763	−0.0013
(2, 3, 3)	1.8239( 56)	0.8443( 90)	2–5	0.132	1.8175	0.0064
(3, 3, 3)	1.9607( 93)	0.8197(154)	2–5	0.000	1.9442	0.0165

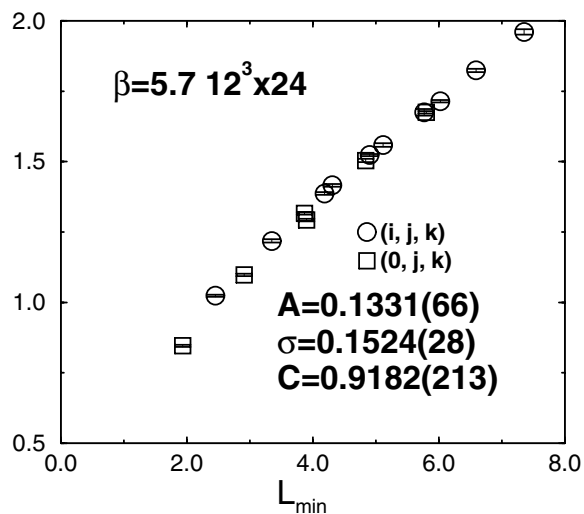


FIG. 3. The  $3Q$  ground-state potential  $V_{3Q}$  as the function of  $L_{\min}$  which is the minimum value of the total length of the flux tubes.

fitting,  $\chi^2$  seems relatively large as  $\chi^2/N_{\text{DF}} = 3.76$ , which may reflect a systematic error on the finite lattice spacing.

We add in Table II the comparison of the lattice data  $V_{3Q}^{\text{latt}}$  with the fitting function  $V_{3Q}^{\text{fit}}$  in Eq. (6) with the parameters listed in Table I. The three-quark ground-state potential  $V_{3Q}$  is well described by Eq. (6) with accuracy better than a few percent.

Next we compare the coefficients  $(\sigma_{3Q}, A_{3Q}, C_{3Q})$  in the  $3Q$  potential  $V_{3Q}$  in Eq. (6) with  $(\sigma_{Q\bar{Q}}, A_{Q\bar{Q}}, C_{Q\bar{Q}})$  in the  $Q\bar{Q}$  potential  $V_{Q\bar{Q}}$  in Eq. (5) as listed in Table I. As a remarkable fact, we find a universal feature of the string tension,  $\sigma_{3Q} \approx \sigma_{Q\bar{Q}}$ , as well as the OGE result for the Coulomb coefficient,  $A_{3Q} \approx \frac{1}{2}A_{Q\bar{Q}}$ .

As a check, we consider the diquark limit, where two quark locations coincide in the  $3Q$  system. In the diquark limit, the static  $3Q$  system becomes equivalent to the  $Q\bar{Q}$  system, which leads to a physical requirement on the relation between  $V_{3Q}$  and  $V_{Q\bar{Q}}$ . Our results,  $\sigma_{3Q} \approx \sigma_{Q\bar{Q}}$  and  $A_{3Q} \approx \frac{1}{2}A_{Q\bar{Q}}$ , are consistent with the physical requirement in the diquark limit. Here the constant term is to be considered carefully in the diquark limit, because there appears a singularity or a divergence from the Coulomb term in  $V_{3Q}$  in the continuum diquark limit,  $\lim_{\mathbf{r}_j \rightarrow \mathbf{r}_i} \frac{-A_{3Q}}{|\mathbf{r}_i - \mathbf{r}_j|} = -\infty$ . In the lattice regularization, this ultraviolet divergence is regularized to be a finite constant with the lattice spacing  $a$  as  $\frac{-A_{3Q}}{|\mathbf{r}_i - \mathbf{r}_j|} \rightarrow \frac{-A_{3Q}}{\omega a}$ , where  $\omega$  is a dimensionless constant satisfying  $0 < \omega < 1$  and  $\omega \sim 1$ . Then, we find  $C_{3Q} + \frac{-A_{3Q}}{\omega a} = C_{Q\bar{Q}}$ , i.e.,  $C_{3Q} - C_{Q\bar{Q}} = \frac{A_{3Q}}{\omega a} (>0)$  in the diquark limit. This is the requirement for the constant term in the diquark limit on the lattice. Our lattice QCD results for  $C_{3Q}$ ,  $C_{Q\bar{Q}}$ , and  $A_{3Q}$  are thus consistent with this requirement, and one finds  $\omega \approx 0.46$ .

Finally, we also try to fit  $V_{3Q}^{\text{latt}}$  with the  $\Delta$ -type flux-tube ansatz of  $V_{3Q} = -A_{\Delta} \sum_{i<j} \frac{1}{|\mathbf{r}_i - \mathbf{r}_j|} + \sigma_{\Delta} \sum_{i<j} |\mathbf{r}_i - \mathbf{r}_j| + C_{\Delta}$ , which was suggested in Refs. [8,10,12]. However, this fitting seems rather worse, because  $\chi^2$  is unacceptably large as  $\chi^2/N_{\text{DF}} = 10.1$  even for the best fit with  $A_{\Delta} = 0.1410(64)$ ,  $\sigma_{\Delta} = 0.0858(16)$ , and  $C_{\Delta} = 0.9344(210)$  in the lattice unit. As an approximation,  $V_{3Q}$  seems described by a simple sum of the effective two-body  $Q\bar{Q}$  potential with a reduced string tension as  $\sigma_{Q\bar{Q}} \approx 0.53\sigma$ . This reduction factor can be naturally understood as a geometrical factor rather than the color factor, since the ratio between  $L_{\min}$  and the perimeter length  $L_P$  satisfies  $\frac{1}{2} \leq L_{\min}/L_P \leq 1/\sqrt{3}$ , which leads to  $L_{\min}\sigma = L_P\sigma_{Q\bar{Q}}$  with  $\sigma_{Q\bar{Q}} = (0.5 \sim 0.58)\sigma$ .

We have studied the static  $3Q$  ground-state potential in SU(3) lattice QCD at the quenched level, using the smearing technique for ground-state enhancement. We have found that  $V_{3Q}$  is well described by a sum of a constant, the two-body Coulomb term, and the three-body linear confinement term  $\sigma_{3Q}L_{\min}$ , where  $L_{\min}$  denotes the minimal length of the color flux tube linking the three quarks. We have also found a universal feature of the string tension as  $\sigma_{3Q} \approx \sigma_{Q\bar{Q}}$ , and the OGE result for Coulomb coefficients as  $A_{3Q} \approx \frac{1}{2}A_{Q\bar{Q}}$ . In lattice QCD studies, however, there appear systematic errors relating to the finite lattice-spacing effect and so on. To obtain the conclusive result on the  $3Q$  potential, we are investigating with finer lattices with large  $\beta$ 's.

- [1] H. Suganuma, H. Matsufuru, Y. Nemoto, and T. T. Takahashi, Nucl. Phys. **A680**, 159 (2000).
- [2] N. Brambilla, G. M. Prosperi, and A. Vairo, Phys. Lett. B **362**, 113 (1995).
- [3] M. Fable de la Ripelle and Yu. A. Simonov, Ann. Phys. (N.Y.) **212**, 235 (1991).
- [4] S. Capstick and N. Isgur, Phys. Rev. D **34**, 2809 (1986).
- [5] W. Lucha, F. F. Schöberl, and D. Gromes, Phys. Rep. **200**, 127 (1991).
- [6] G. S. Bali and K. Schilling, Phys. Rev. D **46**, 2636 (1992).
- [7] K. Schilling, Nucl. Phys. (Proc. Suppl.) **B83-84**, 140 (2000), and references therein.
- [8] R. Sommer and J. Wosiek, Phys. Lett. **149B**, 497 (1984); Nucl. Phys. **B267**, 531 (1986).
- [9] J. Kamesberger *et al.*, in *Proceedings of the Conference on Few-Body Problems in Particle, Nuclear, Atomic and Molecular Physics, Fontevraud, 1987* (Springer-Verlag, New York, 1987), p. 529.
- [10] H. B. Thacker, E. Eichten and J. C. Sexton, Nucl. Phys. (Proc. Suppl.) **B4**, 234 (1988).
- [11] G. S. Bali, e-print hep-ph/0001312, 2000.
- [12] J. M. Cornwall, Phys. Rev. D **54**, 6527 (1996).
- [13] APE Collaboration, M. Albanese *et al.*, Phys. Lett. B **192**, 163 (1987).
- [14] G. S. Bali, C. Schlichter, and K. Schilling, Phys. Rev. D **51**, 5165 (1995).
- [15] J. Kogut and L. Susskind, Phys. Rev. D **11**, 395 (1975).